

Metallosupramolecular helices constructed from nickel(II) and multidentate “click” triazole ligands

Uttam R. Pokharel^{a,b}, Jordan C. Theriot^{b,1}, Frank R. Fronczek^b, Andrew W. Maverick^{b,*}

^a Department of Chemistry and Physical Sciences, Nicholls State University, Thibodaux, LA 70301, USA

^b Department of Chemistry, Louisiana State University, Baton Rouge, LA 70803, USA



ARTICLE INFO

Article history:

Received 20 June 2020

Accepted 15 September 2020

Available online 19 September 2020

Keywords:

Supramolecular coordination

Binuclear triple helicate

Pyridyltriazole

Aminomethyltriazole

Nickel(II)

ABSTRACT

A series of binuclear metallosupramolecular helices $[\text{Ni}_2\text{L}_3]^{4+}$ has been synthesized from Ni(II) salts and bis(bidentate) pyridyltriazole or aminomethyltriazole ligands, separated by *ortho*- (*o*-xpt and *o*-xamt, respectively), *meta*- (*m*-xpt, *m*-xamt), and *para*-xylylene (*p*-xpt, *p*-xamt) spacers. All complexes were characterized by elemental analysis, ESI-MS, and in four cases, the structures confirmed by X-ray crystallography. The xpt and xamt ligands, derived by “click” reactions, exhibit similar bonding behavior regardless of modifications in their coordination pockets and spacer groups, forming triple-helical binuclear complexes with pseudo-octahedral geometry at Ni. The crystallographically characterized complexes show shorter Ni...Ni separations with the *ortho* spacer ($[\text{Ni}_2(\text{o-xpt})_3]^{4+}$, 9.332(2); $[\text{Ni}_2(\text{o-xamt})_3]^{4+}$, 8.9718(10) Å) than with the *para* spacer ($[\text{Ni}_2(\text{p-xpt})_3]^{4+}$, 11.574(2); $[\text{Ni}_2(\text{p-xamt})_3]^{4+}$, 11.899(2), 11.924(2) Å).

© 2020 Elsevier Ltd. All rights reserved.

1. Introduction

Metal-directed self-assembly of transition metal ions and polytopic ligands has been an emerging field of coordination chemistry: unusual shapes of molecules such as helicates, boxes, rings, catenates, and cages can be synthesized from relatively simple starting materials [1–7]. In particular, tetracationic, triple-helical binuclear transition-metal supramolecules are an attractive area in recent years owing to their potential applications as therapeutic agents in the treatment of cancer [8–12] and Alzheimer's disease [13]. These helices are designed considering the structure of the bridging groups, the coordination pockets of the ligand, stereochemical preferences of the metal ions, and non-covalent interactions. Careful choice of the linker group and the coordination behavior of the metal ion can control the overall dimensions of supramolecular aggregates [5]. While many different metal–ligand combinations have been studied for the self-assembly of supramolecular triple-helical complexes, the most common is the nickel(II)–pyridine complexation. These helical polynuclear complexes can be assembled from Ni(II) and oligobipyridine or quaterpyridine ligands; however, synthesis of the ligands is tedious and

time consuming [14–16]. As such, there is still a need for similar binucleating ligands that can be prepared by mild and modular methods. As an analog of bipyridines, pyridyltriazoles have received tremendous attention owing to their high efficiency of synthesis, ease of purification, functional group tolerance, and compatibility with various solvents. Pyridyltriazoles are readily synthesized by the copper-catalyzed Huisgen azide-alkyne cyclization (a “click” reaction) [17,18].

Our research group has long been involved [19–21] in designing discrete macrocyclic metal–organic compounds based on Cu(II) and multifunctional organic linkers. We have recently studied the self-assembly of metallosupramolecular cages from tetradentate bis(pyridyltriazole) ligands, separated with aromatic spacers, and Cu(II) to capture bifunctional Lewis-basic guests [22,23]. The most common coordination numbers in copper(II) complexes are 4 and 5. Thus, when Cu(II) reacts with a tetradentate binucleating ligand LL, the most stable products have a metal:ligand ratio of 2:2, i.e. $[\text{Cu}_2(\text{LL})_2]$ (Fig. 1a), with approximately square-planar coordination [24] as well as square-pyramidal species such as $[\text{Cu}_2(\text{LL})_2\text{X}_2]^{2+}$ (Fig. 1b) [22]. As an extension of the work, we were also interested in studying metallosupramolecular cages with the $[\text{Ni}_2(\text{LL})_3]^{4+}$ stoichiometry. Although the complexation of pyridyltriazole ligands with transition metal ions has been studied extensively [25], aminomethyltriazole ligands are still relatively new. There are limited examples of 1:1 complexation of aminomethyltriazoles with Pd(II), Pt(II), Tc(I), and Re(I) [26–28].

* Corresponding author.

E-mail address: maverick@lsu.edu (A.W. Maverick).

¹ Present address: Department of Chemistry and Biochemistry, University of Colorado, Boulder, CO, USA.

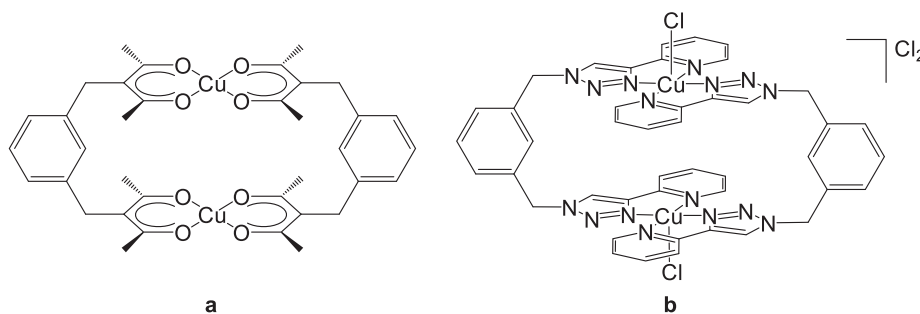


Fig. 1. Supramolecular assembly of tetradentate ligands with Cu(II) often produces (a) four-coordinate or (b) five-coordinate complexes.

When a pyridyltriazole ligand coordinates to metal ions that have square-planar geometrical preferences, the coordination sometimes deviates slightly from ideal square-planar geometry, e.g. by twisting of the ligands [22]. This might be due to steric hindrance between the H atom of a pyridyl group and the triazole ring of another ligand (Fig. 2a).

When the pyridyl moieties are replaced by aminomethyl groups, the hydrogen atoms of the amino groups lie out of the coordination plane (Fig. 2b), potentially reducing inter-ligand repulsions. This kind of comparison has been made in other families of ligands, such as with 2,2'-bipyridine and 2-(aminomethyl)pyridine. In addition, the presence of amino groups in the ligands can improve the solubility of complexes in protic media due to hydrogen bonding with the solvent.

Mononuclear complexes ML_3 with bidentate chelating ligands generally have idealized D_3 symmetry, with enantiomers designated P (or Δ) and M (or Λ) [29–32]. Analogous dimeric complexes constructed from bis(bidentate) ligands LL, i.e. $[M_2(LL)_3]^{n+}$, can be either homochiral (with P,P and M,M enantiomers, each having idealized D_3 symmetry) or achiral (with one metal P and the other M , and idealized C_{3h} symmetry) [29,30,33]. The homochiral diastereomers are called *helicates*, because the screw sense is the same at both metals; the P,M diastereomer is called a *mesocate*. The helicate and mesocate diastereomers of $[M_2(LL)_3]^{n+}$ are illustrated schematically in Fig. 3.

Our current focus is to investigate the self-assembly of flexible tetradentate bis(pyridyltriazole) or bis(aminomethyltriazole) ligands, separated with *ortho*-, *meta*-, and *para*-xylylene spacers (Chart 1), and Ni(II) to see the effects of change in the aromatic core as well as coordination pockets in determining the final topology of the supramolecular architecture. Although complexes of *ortho*- [17,34], *meta*- [17,22,35–37], and *para*- [17,29,30,35,37–39] xylylenebis(pyridyltriazole) ligands have been reported for different transition metals, as far as we are aware, no metal complexes of tetradentate bis(aminomethyltriazole) ligands have been reported. Herein we report the synthesis and characterization, including molecular structures, of triple-helical Ni(II) complexes constructed with the three isomeric xylylenebis(pyridyltriazole) and xylylenebis(aminomethyltriazole) ligands and Ni(II) salts.

2. Experimental section

2.1. Materials and analyses

All chemicals were reagent grade obtained from commercial sources and used without further purification. Microanalyses (C, H, N) were performed by M-H-W laboratories, Phoenix, Arizona. 1H NMR and ^{13}C NMR spectra were recorded on a Varian Inova spectrometer (1H , 500 MHz; ^{13}C , 125 MHz) at ca. 22 °C and were referenced to residual solvent peaks. The ESI-MS (electrospray mass spectra) were acquired on an Agilent 6210 instrument. The

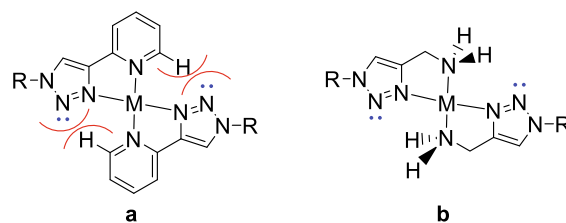


Fig. 2. (a) A *trans*-bis(pyridyltriazole) complex showing unfavorable triazole-H(C) interactions that could lead to structural distortion; (b) a *trans*-bis(aminomethyltriazole) complex which avoids such repulsive interactions by replacing pyridyl moieties with aminomethyl groups.

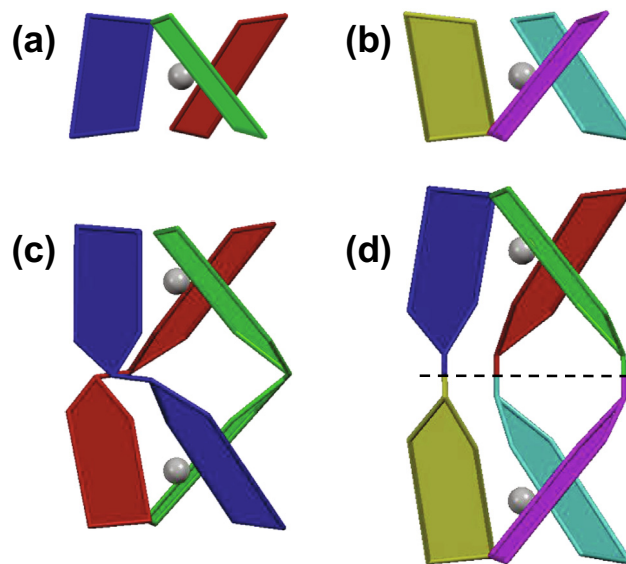


Fig. 3. Schematic illustration of the two enantiomers of a mononuclear complex $[ML_3]^{n+}$, with colored planes representing chelating ligands, and their assembly into helicate and mesocate forms $[M_2(LL)_3]^{n+}$. (a) The M enantiomer of a mononuclear complex $[ML_3]^{n+}$; (b) the P enantiomer of $[ML_3]^{n+}$, represented by different ligand colors; (c) the MM diastereomer of a binuclear complex $[M_2(LL)_3]^{n+}$, a helicate, with the same chirality (and the same color scheme) at both metals; and (d) the MP diastereomer of $[M_2(LL)_3]^{n+}$, a mesocate, with opposite chirality (and different color schemes) at the two metals, and a mirror plane (---) in the center.

boc-protected *meta*-, and *para*-xylylenebis(aminomethyltriazole) were synthesized by following the procedure reported by the Haridas group [40] and the procedure was extended to synthesize boc-protected *ortho*-xylylenebis(aminomethyltriazole), as described below. *Caution*: Organic azides may be explosive under certain conditions. We did not experience any difficulties in working with the xylylenebis(azides) required for the aminomethyltriazole preparations. However, we did not prepare them in quantities larger than

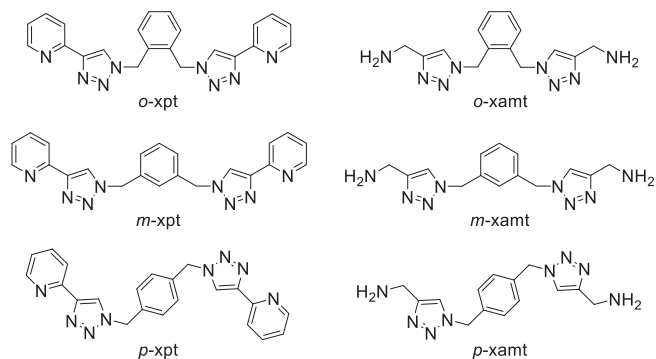


Chart 1. Xylylenebis(pyridyltriazole) and xylylenebis(aminomethyltriazole) ligands.

that given here, and we handled them only behind a hood sash or a safety shield.

2.2. Synthesis of *o*-xylylenebis(*boc*-aminomethyltriazole)

To a stirred solution of *boc*-propargylamine (2.53 g, 16.4 mmol) in dry acetonitrile (25 mL) at 0 °C, diisopropylethylamine (DIEA) (3.13 mL, 18.8 mmol) and *o*-xylylenebis(azide) [41] (1.40 g, 7.45 mmol) were added under nitrogen. CuI (146 mg, 0.77 mmol) was added and the reaction mixture stirred for 16 h at room temperature. A white suspension formed. The volatiles were removed *in vacuo*, and the solid mass was dissolved in chloroform and extracted with a solution (100 mL) prepared from concentrated NH₃(aq) (10.0 mL) and ammonium chloride (1.00 g) in water. The organic layer was collected and washed successively with H₂SO₄ (4 M), saturated NaHCO₃(aq), and water. The organic layer was dried with anhydrous MgSO₄, filtered, and the filtrate evaporated to dryness. The product was purified by trituration with cold diethyl ether to give *o*-xylylenebis(*boc*-aminomethyltriazole) (3.42 g, 92%) as a white solid, mp: 185 °C. ¹H NMR (CDCl₃): δ 1.39 (s, 18H, (CH₃)₃), 4.34 (d, 4H, ³J = 6.0 Hz, NHCH₂), 5.28 (br, 2H, NHCH₂), 5.58 (s, 4H, CH₂), 7.27 (d, ³J = 7.5 Hz, 2H, Ar), 7.29 (d, ³J = 7.5 Hz, 2H, Ar), 7.45 (s, 4H, Ar). ¹³C NMR (CDCl₃): δ 28.5, 36.3, 51.4, 79.9, 122.0, 129.9, 130.6, 133.4, 146.5, 156.1.

2.3. General method of preparation of the xylylenebis(aminomethyltriazoles) *o*-xamt, *m*-xamt, and *p*-xamt via their HCl salts

The *boc*-protected xylylenebis(aminomethyltriazole) (2.0 g, 4.0 mmol) was dissolved in a mixture of conc. HCl(aq) and methanol (1:5 v/v) (20 mL), and heated to reflux for 12 h. A white suspension was formed. The reaction mixture was cooled to room temperature and filtered. The residue was washed with cold methanol and dried.

2.3.1. *o*-xamt·2HCl

Yield 87%; ¹H NMR (D₂O): δ 4.27 (s, 4H, CH₂), 5.72 (s, 4H, CH₂), 7.40 (d, ³J = 7.6 Hz, 2H, Ar), 7.51 (d, 2H, ³J = 7.6 Hz, Ar), 8.00 (s, 2H, triazole-H). This product (500 mg, 1.35 mmol) was dissolved in 6 M NaOH(aq) (10 mL) and extracted with dichloromethane (3 × 50 mL). The organic layer was dried with MgSO₄, filtered, and the filtrate evaporated to dryness to give *o*-xamt (102 mg, 25%) as a white solid, mp 59 °C. ¹H NMR (DMSO *d*₆): δ 3.74 (br, 4H, CH₂), 5.76 (s, 4H, CH₂), 7.14 (d, ³J = 7.5 Hz, 2H, Ar), 7.34 (d, ³J = 7.5 Hz, 2H, Ar), 7.85 (s, 2H, triazole CH). ¹³C NMR (DMSO *d*₆): δ 37.2, 49.7, 122.1, 128.7, 129.1, 134.3, 150.2.

2.3.2. *m*-xamt·2HCl

Yield 91%; ¹H NMR (D₂O): δ 4.32 (s, 4H, CH₂), 5.63 (s, 4H, CH₂), 7.25 (s, 1H, Ar), 7.32 (d, 2H, ³J = 7.5 Hz, Ar), 7.44 (t, 1H, ³J = 7.5 Hz, Ar), 8.14 (s, 2H, triazole CH). ESI-MS: *m/z* 299.1729 [M - 2HCl + H]⁺ (calcd 299.1733), 597.3378 [2M - 4HCl + H]⁺ (calcd 597.3387). The salt (200 mg, 0.54 mmol) was dissolved in 6 M aqueous NaOH (10 mL) and extracted with chloroform (2 × 20 mL). The organic layer was dried with MgSO₄, filtered, and the filtrate evaporated to dryness to give *m*-xamt (139 mg, 86%) as a white solid, mp: 82 °C. ¹H NMR (CDCl₃): δ 1.64 (br, 4H, NH₂), 3.96 (s, 4H, CH₂), 5.48 (s, 4H, CH₂), 7.16 (s, 1H, Ar), 7.24 (d, 2H, ³J = 8.2 Hz, Ar), 7.35 - 7.38 (m, 3H, 1 Ar + 2 triazole CH). ¹³C NMR (CDCl₃): δ 37.9, 53.8, 105.2, 120.8, 127.7, 128.5, 136.1, 150.3.

2.3.3. *p*-xamt·2HCl

Yield 75%; ¹H NMR (D₂O): δ 4.33 (s, 4H, CH₂), 5.65 (s, 4H, CH₂), 7.36 (s, 4H, Ar), 8.15 (s, 2H, triazole CH). ESI-MS: *m/z* 299.1703 [M - 2HCl + H]⁺ (calcd 299.1733), 597.3315 [2M - 4HCl + H]⁺ (calcd 597.3387). The product (200 mg, 0.54 mmol) was dissolved in 10% aqueous NaOH (10 mL) and extracted with chloroform (2 × 20 mL). The organic layer was dried with MgSO₄, filtered, and the filtrate evaporated to dryness to give *p*-xamt (152 mg, 94%) as a white solid, mp 162 °C. ¹H NMR (CDCl₃): δ 3.96 (s, 4H, CH₂), 5.49 (s, 4H, CH₂), 7.27 (s, 4H, Ar), 7.35 (2H, triazole CH). ¹³C NMR (CDCl₃): δ 37.8, 53.8, 120.6, 120.9, 128.8, 129.1, 135.6.

2.4. Synthesis of Ni(II) xpt complexes **1a–3a**

To a stirred solution of Ni(BF₄)₂·6H₂O (58 mg, 0.17 mmol) in methanol (20 mL), the xpt ligand (100 mg, 0.25 mmol) dissolved in chloroform (20 mL) was added dropwise. The reaction mixture was stirred for 3 h at room temperature. The precipitate was separated by filtration and washed with chloroform and methanol to give a pink powder. Vapor diffusion of ethyl ether into solutions of **1a** and **3a** in DMF gave pink crystalline solids suitable for analysis by X-ray crystallography.

2.4.1. [Ni₂(*o*-xpt)₃](BF₄)₄ (**1a**)

Yield 70%; ESI-MS: *m/z* 1557.3829 [Ni₂(*o*-xpt)₃(BF₄)₃]⁺ (calcd 1557.3825), 735.1881 [Ni₂(*o*-xpt)₃(BF₄)₂]²⁺ (calcd 735.1898), 461.4566 [Ni₂(*o*-xpt)₃(BF₄)₃]³⁺ (calcd 461.4573), 324.5919 [Ni₂(*o*-xpt)₃]⁴⁺ (calcd 324.5912). Anal. Calcd for C₆₆H₅₄B₄F₁₆N₂₄Ni₂·3CHCl₃: C, 41.31, H 2.86, N 16.76. Found: C 41.28, H 2.82, N 16.24.

2.4.2. [Ni₂(*m*-xpt)₃](BF₄)₄ (**2a**)

Yield 77%; ESI-MS: *m/z* 324.5928 [Ni₂(*m*-xpt)₃]⁴⁺ (calcd 324.5912). Anal. Calcd. for C₆₆H₅₄B₄F₁₆N₂₄Ni₂·CHCl₃·2DMF: C 45.82, H 3.63, N 19.03. Found: C 46.53, H 3.78, N 19.01.

2.4.3. [Ni₂(*p*-xpt)₃](BF₄)₄ (**3a**)

Yield 78%; ESI-MS: 735.1749 [Ni₂(*p*-xpt)₃(BF₄)₂]²⁺ (calcd 735.1898), 461.4552 [Ni₂(*p*-xpt)₃(BF₄)₃]³⁺ (calcd 461.4573), 324.5935 [Ni₂(*p*-xpt)₃]⁴⁺ (calcd 324.5912). Anal. Calcd. for C₆₆H₅₄B₄F₁₆N₂₄Ni₂·2CHCl₃·2DMF: C 43.72, H 3.47, N 17.91. Found: C 43.64, H 3.43, N 18.17.

2.5. Synthesis of complexes **1b** and **2b**

To a stirred solution of *o*- or *m*-xamt·2HCl (100 mg, 0.27 mmol) in water (5 mL), Ni(BF₄)₂·6H₂O (61 mg, 0.17 mmol) and triethylamine (2.0 mL) was added. The reaction mixture was stirred for 3 h at room temperature and filtered, and excess NH₄PF₆ was added to the filtrate. The resulting precipitate was collected and rinsed with water to give a pink powder. Vapor diffusion of ethyl ether into a solution of **1b** in DMF or MeCN gave pink crystalline solid suitable for analysis for X-ray crystallography.

2.5.1. $[\text{Ni}_2(o\text{-xamt})_3](\text{PF}_6)_4$ (**1b**)

Yield 68%. Anal. Calcd. for $\text{C}_{42}\text{H}_{54}\text{F}_{24}\text{N}_{24}\text{Ni}_2\text{P}_4\cdot 2\text{CH}_3\text{CN}$: C 33.00, H 3.61, N 21.75. Found: C 32.86, H 3.70, N 21.36.

2.5.2. $[\text{Ni}_2(m\text{-xamt})_3](\text{PF}_6)_4$ (**2b**)

Yield 61%; ESI-MS: m/z 1445.2544 $[\text{Ni}_2(m\text{-xamt})_3](\text{PF}_6)_3]^+$ (Calcd. 1445.2590), 650.1389 $[\text{Ni}_2(m\text{-xamt})_3](\text{PF}_6)_2]^{2+}$ (calcd 650.1471), Anal. Calcd. for $\text{C}_{42}\text{H}_{54}\text{F}_{24}\text{N}_{24}\text{Ni}_2\text{P}_4\cdot 2\text{H}_2\text{O}$: C 31.68, H 3.42, N 21.11. Found C 31.56, H 3.40, N 21.01.

2.5.3. Synthesis of $[\text{Ni}_2(p\text{-xamt})_3](\text{NO}_3)_4$ (**3b**)

To a stirred solution of $\text{Ni}(\text{NO}_3)_2\cdot 6\text{H}_2\text{O}$ (64 mg, 0.22 mmol) in methanol (10 mL), *p*-xamt (100 mg, 0.33 mmol) in chloroform (10 mL) was added slowly. The reaction mixture was stirred for 3 h, and the resulting precipitate was collected by filtration to give **3b** (92 mg, 66%) as a light pink solid. The product was crystallized from its solution in DMF by vapor diffusion of diethyl ether. ESI-MS: m/z 1196.3255 $[\text{Ni}_2(p\text{-xamt})_3](\text{NO}_3)_3]^+$ (Calcd 1196.3299). Anal. Calcd. for $\text{C}_{54}\text{H}_{82}\text{N}_{32}\text{Ni}_2\text{O}_{16}\cdot 4\text{DMF}$: C 41.77, H 5.32, N 28.86. Found: C 41.68, H 5.34, N 28.79.

2.6. X-ray analyses

Intensity data were collected at low temperature on a Bruker Kappa Apex-II DUO CCD diffractometer fitted with an Oxford Cryostream chiller. Radiation was from a $\text{CuK}\alpha$ source ($1\mu\text{S}$ microfocus tube with QUAZAR multilayer optics). Data reduction included absorption corrections by the multiscan method, with SADABS [42]. The structures were determined by direct methods and difference Fourier techniques and refined by full-matrix least squares, using SHELXL [43]. All non-hydrogen atoms were refined anisotropically, except for a disordered phenyl group and a disordered BF_4^- ion in **1a** and partially populated water molecules in **3b**. Disordered solvent molecules were removed using the SQUEEZE procedure [44] for all compounds except **1b**; in **3b**, reasonable models for four of the eight independent nitrate ions could not be refined, so they were also removed with SQUEEZE. In the final model for **1a**, the disordered phenyl had two conformations with occupancies 0.557(16)/0.443(16), and one BF_4^- ion was disordered in two orientations with 0.533(10)/0.467(10) occupancies by rotation about a B-F vector. In **1b**, two PF_6^- anions were similarly disordered by rotation about F-P-F lines. In one, the two occupancies were 0.815(9)/0.185(9), and in the other they were 0.639(12)/0.361(12). In **3b**, one DMF molecule was disordered into two orientations with occupancies 0.595(11)/0.405(11), and this disorder is correlated with two partially populated water molecules. All H atoms were placed in idealized positions, except for those in water molecules in **3b**, which could not be located. In **1b**, the Ni dimer lies on an approximate twofold axis, and the structure is pseudosymmetric to C_2/c . It is an inversion twin with population of the two components 0.646(18)/0.354(18). For additional details, see Table 1.

3. Results and discussion

3.1. Synthesis of ligands

The tetradentate *N*-donating ligands used in the current studies are depicted in Chart 1. The pyridyltriazole ligands, *o*-xpt, *m*-xpt and *p*-xpt, were synthesized by the [3 + 2] cycloaddition reaction of 2-ethynylpyridine with *in situ* generated diazides by the copper-catalyzed azide-alkyne cycloaddition (CuAAC; “click” reaction) [17]. We attempted to use this method to synthesize boc-protected xylylenebis(aminomethyltriazoles), but it gave very poor yields. Therefore, we first converted the xylylene dibromides to the corre-

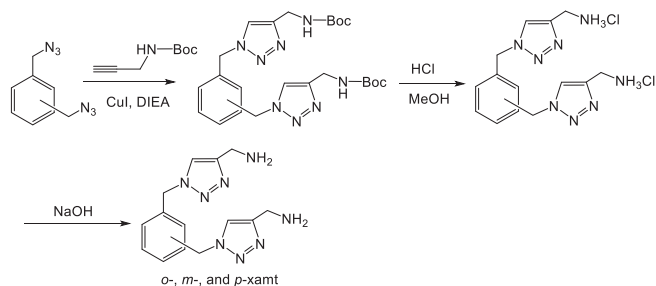
Table 1

Crystal data and structure refinement for compounds **1a**, **3a**, **1b** and **3b**.

Compound	1a [Ni ₂ (<i>o</i> -xpt) ₃] (BF ₄) ₄ ·CHCl ₃	3a [Ni ₂ (<i>p</i> -xpt) ₃] (BF ₄) ₄ ·3DMF
CCDC deposition number	2010484	2010486
formula	C ₆₇ H ₅₅ B ₄ Cl ₃ F ₁₆ N ₂₄ Ni ₂	C ₇₅ H ₇₅ B ₄ F ₁₆ N ₂₇ Ni ₂ O ₃
mw	1767.36	1867.28
crystal system	Monoclinic	Monoclinic
space group	<i>P</i> 2 ₁ / <i>n</i>	<i>P</i> 2 ₁ / <i>c</i>
<i>a</i> /Å	12.5605(7)	25.3000(14)
<i>b</i> /Å	16.6264(10)	15.0624(8)
<i>c</i> /Å	47.126(3)	24.5532(14)
β/deg	95.049(4)	111.075(3)
<i>V</i> /Å ³	9803.4(10)	8730.8(9)
<i>Z</i>	4	4
<i>T</i> /K	90.0(5)	90.0(5)
<i>D</i> _{calc} /g cm ⁻³	1.197	1.421
cryst dimen/mm	0.05 × 0.25 × 0.40	0.08 × 0.12 × 0.17
θ limits, deg	3.735–60.063	3.481–62.626
reflms, measd/unique/obsd	32785/14007/11894	55904/13804/9255
<i>F</i> (000)	3584	3832
μ/mm ⁻¹	1.901	1.376
<i>R</i> _{int}	0.0402	0.0836
<i>R</i> [<i>I</i> > 2σ(<i>I</i>)]	0.1189	0.0829
<i>R</i> _w (all data)	0.3317	0.2395
GOF	1.041	1.033

Compound	1b [Ni ₂ (<i>o</i> -xamt) ₃] (PF ₆) ₄ ·5CH ₃ CN	3b [Ni ₂ (<i>p</i> -xamt) ₃] (NO ₃) ₄ ·1.5DMF·0.76H ₂ O
CCDC deposition number	2010485	2010487
formula	C ₅₂ H ₆₉ F ₂₄ N ₂₉ Ni ₂ P ₄	C _{46.5} H _{66.02} N _{29.5} Ni ₂ O _{14.26}
mw	1797.66	1383.69
crystal system	Monoclinic	Monoclinic
space group	<i>Cc</i>	<i>P</i> 2 ₁ / <i>n</i>
<i>a</i> /Å	28.3349(16)	30.0989(19)
<i>b</i> /Å	12.3518(7)	12.7391(17)
<i>c</i> /Å	22.6035(12)	34.642(2)
β/deg	109.023(2)	109.292(3)
<i>V</i> /Å ³	7478.9(7)	12537.0(13)
<i>Z</i>	4	8
<i>T</i> /K	90.0(5)	90.0(5)
<i>D</i> _{calc} /g cm ⁻³	1.597	1.593
cryst dimen/mm	0.27 × 0.20 × 0.14	0.04 × 0.12 × 0.39
θ limits, deg	3.30–67.57	2.374–66.645
reflms, measd/unique/obsd	23950/10751/10541	56208/21540/15704
<i>F</i> (000)	3664	6248
μ/mm ⁻¹	2.499	1.613
<i>R</i> _{int}	0.0260	0.0429
<i>R</i> [<i>I</i> > 2σ(<i>I</i>)]	0.0407	0.0628
<i>R</i> _w (all data)	0.1160	0.1921
GOF	1.029	1.027

sponding diazides by reaction with NaN_3 in DMF/ H_2O at room temperature, followed by the “click” reaction between the diazides and boc-propargylamine in the presence of CuI/DIEA [40]. The boc-protected *meta*- and *para*-xylylenebis(aminomethyltriazole) were synthesized by following the procedure reported by the Haridas group [40]; we extended the method to the analogous *ortho* isomer (92% yield). Deprotection was performed by heating the boc-protected amines in the presence of HCl (Scheme 1). The xylylenebis(aminomethyltriazole) ligands were isolated as hydrochloride salts $\text{xamt}\cdot 2\text{HCl}$. ESI-MS analysis of these hydrochloride salts shows peaks corresponding to the protonated free amine, xamtH^+ ($m/z = 299.18$), and its dimer ($m/z = 597.33$). Water solubility of these hydrochloride salts varies in the order *ortho* ≫ *meta* > *para*. Deprotonation with $\text{NaOH}(\text{aq})$, and extraction into organic solvents, afforded the free bases *o*-, *m*-, and *p*-xamt.



Scheme 1. Synthesis of xylylenebis(aminomethyltriazole) dihydrochloride salts and free bases.

3.2. Synthesis of the complexes

The Ni(II) complexes of *o*-, *m*- and *p*-xpt (**1a–3a**) were synthesized by slow addition of ligands (3 equivalents) in chloroform to stirred solutions of Ni(II) salts (2 equivalents) in methanol at room temperature (Scheme 2a). The compounds were isolated in 70–80% yield as pink solids. $[\text{Ni}_2(\text{o-xpt})_3](\text{BF}_4)_4$ (**1a**) and $[\text{Ni}_2(\text{p-xpt})_3](\text{BF}_4)_4$ (**3a**) are readily soluble in DMF, whereas $[\text{Ni}_2(\text{m-xpt})_3](\text{BF}_4)_4$ (**2a**) is less soluble. ESI-MS analysis of the isomeric salts showed weak signals corresponding to $[\text{Ni}_2(\text{xpt})_3](\text{BF}_4)_3^+$ (m/z 1557.38), while the $[\text{Ni}_2(\text{xpt})_3](\text{BF}_4)_2^{2+}$ (m/z 735.19), $[\text{Ni}_2(\text{xpt})_3](\text{BF}_4)^{3+}$ (m/z 461.46), and $[\text{Ni}_2(\text{xpt})_3]^{4+}$ (m/z 324.59) signals were fairly strong. The observed isotopic distributions were in good agreement with calculated values. Additional characterization was performed by microanalysis, and in the case of **1a** and **3a**, by X-ray structure determination.

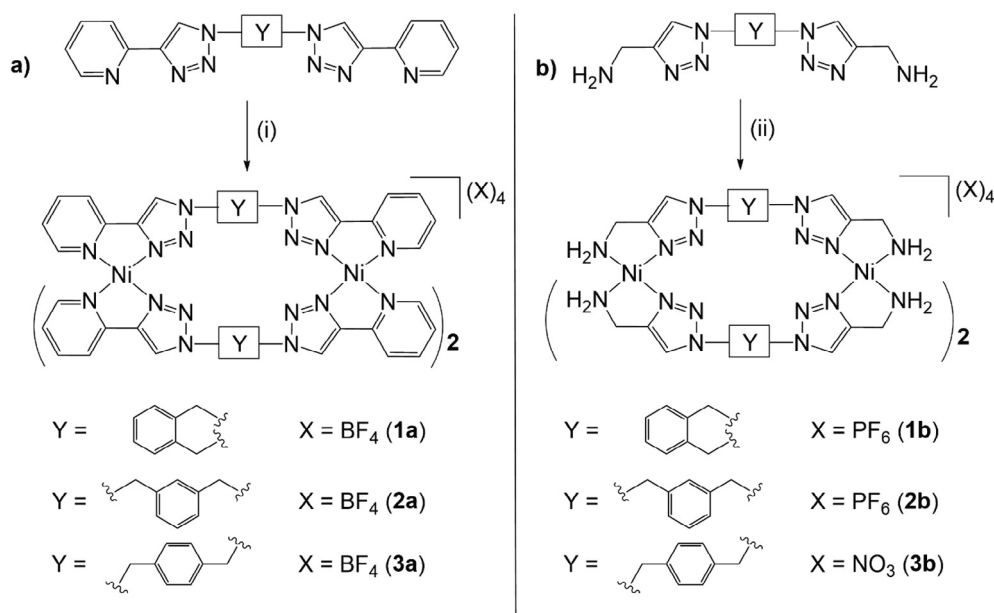
To modify the physical and coordination properties of the bis-chelating “click” ligands, we used the aminomethyl group as a substitute for the pyridyl group. The Ni(II) complexes of *o*- and *m*-xamt were obtained by the treatment of $\text{Ni}(\text{BF}_4)_2 \cdot 6\text{H}_2\text{O}$ with the ligand hydrochloride salts (3:2 ratio) in the presence of excess triethylamine in aqueous medium. To improve the solubility of the complexes in organic solvents, the BF_4 salts were metathesized with ammonium hexafluorophosphate to give pink solids (**1b** and **2b**) in 60–70% overall yield. Because of the poor solubility of *p*-xamt-2HCl in water as well as in organic solvents, the complex

3b was synthesized by first isolating the free amine, *p*-xamt. The coordination of *p*-xamt was achieved by stirring with nickel(II) nitrate (3:2 ratio) in methanol. The microanalyses of all products were consistent with the formation of binuclear complexes $[\text{Ni}_2\text{L}_3]^{4+}$ and the results were further supported by ESI mass analysis. Unlike $\text{Ni}_2(\text{xpt})_3(\text{BF}_4)_4$ complexes, the ESI-MS analysis of $\text{Ni}_2(\text{-xamt})_3(\text{PF}_6)_4$ complexes showed peaks corresponding to only monocationic ($[\text{Ni}_2(\text{xamt})_3](\text{PF}_6)_3^+$; m/z 1445.25) and dicationic ($[\text{Ni}_2(\text{xamt})_3](\text{PF}_6)_2^{2+}$; m/z 650.14) ions.

3.3. X-ray crystallographic studies

X-ray quality crystals were isolated for the complexes **1a**, **3a**, **1b** and **3b**. In all cases, the crystals contained the expected nickel(II) metallosupramolecular helicates $[\text{Ni}_2\text{L}_3]^{4+}$. In all complexes the two metal centers are crystallographically non-equivalent. The complex **3a** has also been crystallographically characterized previously as its BF_4 salt by Petitjean and co-workers [30]. Although we followed similar conditions for reaction and crystallization as the Petitjean group, the previously reported complex crystallizes in the $R\bar{3}c$ space group while our complex **3a** crystallizes in the monoclinic space group $P2_1/c$. The asymmetric unit of complex **3b** includes two crystallographically independent molecules. We were unable to obtain crystals suitable for X-ray crystallography from the *meta* ligands (complexes **2a** and **2b**) despite multiple attempts. The crystal data and structure refinement parameters for the compounds are presented in Table 1.

The cations in the structures are similar (Fig. 4) and confirm the formation of the binuclear triple-helical architectures regardless of change in coordination pockets of the ligands. In each structure, the nickel(II) centers are bound to three pyridyltriazole (**1a** and **3a**) or aminomethyltriazole (**1b** and **3b**) units from three different ligand strands in the *fac* configuration attaining a pseudo-octahedral coordination geometry. In the pyridyltriazole structures (**1a** and **3a**), the triazole rings are approximately coplanar with the adjacent pyridyl units: the torsion angles between the two donor N atoms and bridging C atoms of the pyridyltriazole units are in the range of 3–6°. In contrast, the aminomethyltriazole ligands are more flexible, leading to a wider range of analogous torsion angles (2–33°).



Scheme 2. Synthesis of nickel(II) metallosupramolecular cages $[\text{Ni}_2(\text{LL})_3]\text{X}_4$. Reagents: (a) (i) $\text{Ni}(\text{BF}_4)_2 \cdot 6\text{H}_2\text{O}$; (b) (ii) $\text{Ni}(\text{BF}_4)_2 \cdot 6\text{H}_2\text{O}$ followed by NH_4PF_6 ; or $\text{Ni}(\text{NO}_3)_2 \cdot 6\text{H}_2\text{O}$.

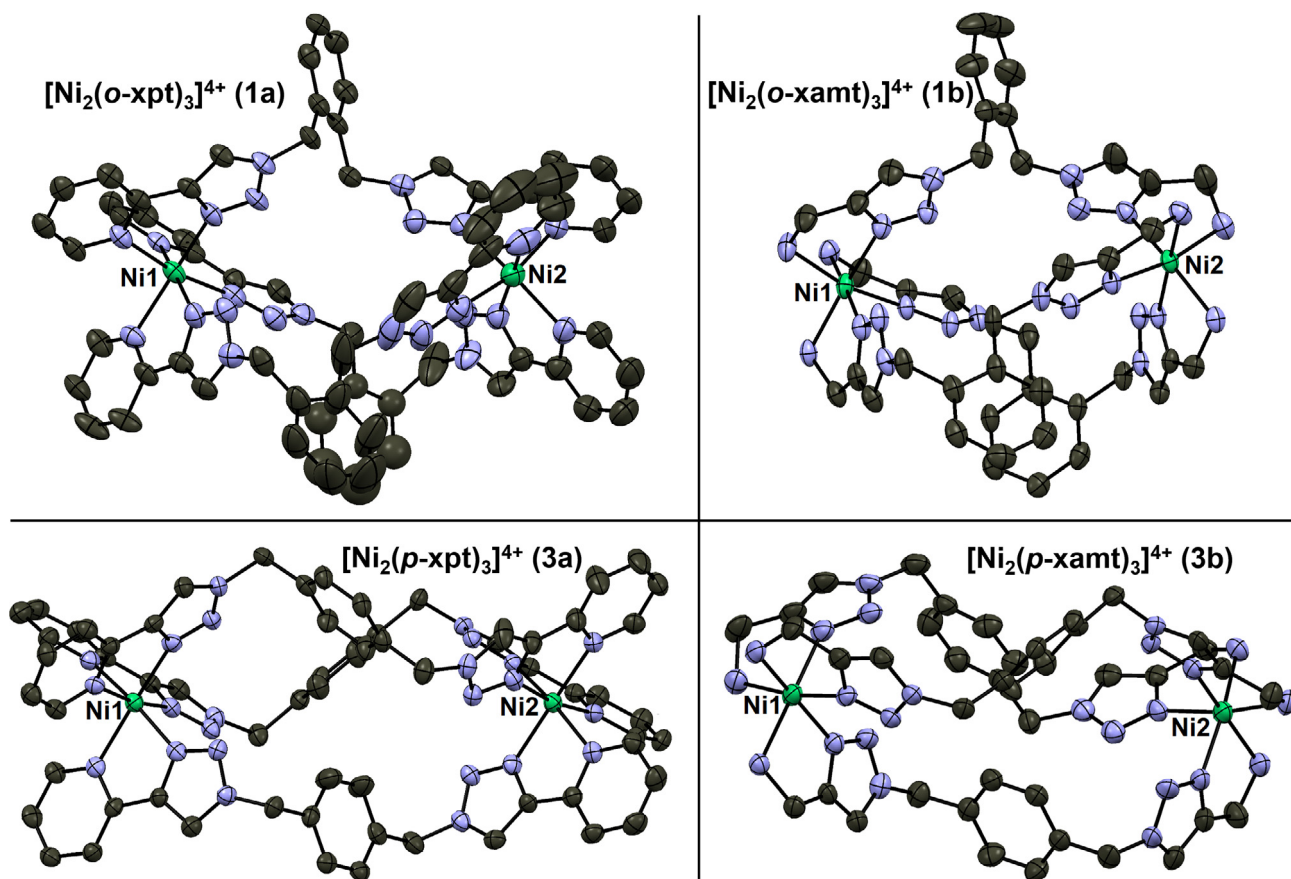


Fig. 4. ORTEP diagrams of the solid state structures of nickel(II) metallosupramolecular helices: **1a**, $[\text{Ni}_2(\text{o-xpt})_3]^{4+}$; **3a**, $[\text{Ni}_2(\text{p-xpt})_3]^{4+}$; **1b**, $[\text{Ni}_2(\text{o-xamt})_3]^{4+}$; **3b**, $[\text{Ni}_2(\text{p-xamt})_3]^{4+}$. Thermal ellipsoids are shown at the 50% probability level. Anions, hydrogen atoms, and solvent molecules have been removed for clarity.

The stereochemistry of the self-assembly process can be influenced by the number of carbon atoms in the spacer groups Y between the two ML_3 moieties [45]. With an odd number of carbon atoms in the two ML_3 units, the complexes usually form as an achiral mesocate (with opposite chirality, P,M , at the two metal atoms, and idealized mirror symmetry). On the other hand, spacer units with an even number of carbon atoms tend to produce helicates, as racemic mixtures of the (P,P) and (M,M) enantiomers. Consistent with the even number of carbon atoms in both o - and p -xylylene groups, all four complexes (**1a**, **3a**, **1b**, and **3b**) crystallize as racemic mixtures of the (P,P) and (M,M) helicates. Despite numerous attempts, we were unable to produce suitable crystals of the complexes from m -xylylene linkers (**2a** and **2b**). However, the published example of $[\text{Fe}_2(m\text{-xpt})_3]^{4+}$ crystallizes as a (P,M) -mesocate [39].

A summary of metal–metal distances and structure types for o -, m -, and p -xylylene-linked pyridyltriazole, aminomethyltriazole, and related complexes is presented in Table 2. The p -linked complexes show longer metal–metal distances, as expected. The $M\cdots M$ distances for the two m -linked complexes are longer still. This order of $M\cdots M$ distances ($o < p < m$) is reproduced by simple molecular modeling calculations (Hyperchem). Models of the helicates suggest that, because the adjacent complexes have the same chirality, the bridging groups can continue the same screw sense as the ligating moieties. This leads to efficient packing and relatively small $M\cdots M$ distances. In contrast, in the mesocates, the chirality changes from M to P at the m -xylylene bridging group, so it is approximately parallel to the $M\cdots M$ axis, leading to a larger separation between the metal atoms. This is seen qualitatively in Fig. 3: the change in chirality in the mesocate interferes with

efficient packing of the two ML_3 moieties. As far as we are aware, the present structures of $[\text{Ni}_2(\text{o-xpt})_3]^{4+}$, $[\text{Ni}_2(\text{o-xamt})_3]^{4+}$ and $[\text{Ni}_2(\text{p-xamt})_3]^{4+}$ are the first of these xylylene-linked $\text{M}_2(\text{LL})_3$ to be reported.

The average Ni–N(pyridine) and Ni–N(triazole) distances, and N(pyridine)–Ni–N(triazole) angles in the $[\text{Ni}_2(\text{xpt})_3]^{4+}$ structures are 2.106(14) and 2.054(14) Å, and 78.7(5)°, respectively. These are very similar to those for analogous structures in the literature: 2.10(5) (5791 hits in 1340 $\text{Ni}(\text{py})_n$ structures) and 2.07(3) Å (33 hits in 11 $\text{Ni}(\text{triazole})_n$ structures), and 78.8(4)° (19 hits in 8 $\text{Ni}(\text{pyridyltriazole})_n$ structures) [46].

The folding of the ligands in these supramolecular structures depends on the nature of the xylylene spacer involved. The com-

Table 2

Structure types and metal–metal distances for $[\text{M}_2(\text{xpt})_3]^{4+}$ and $[\text{M}_2(\text{xamt})_3]^{4+}$ and related species.

Compound	Type	$M\cdots M$ (Å)	Ref
$[\text{Ni}_2(\text{o-xpt})_3](\text{BF}_4)_4$ (1a)	Helicate	9.332(2)	This work
$[\text{Ni}_2(\text{o-xamt})_3](\text{PF}_6)_4$ (1b)	Helicate	8.9718(10)	This work
$[\text{Fe}_2(m\text{-xpt})_3](\text{BF}_4)_4$	Mesocate	12.182(3)	[39]
$[\text{Fe}_2(2,6\text{-pmpt})_3](\text{BF}_4)_4$ ^a	Mesocate	12.234(1)	[39]
$[\text{Ni}_2(\text{p-xpt})_3](\text{BF}_4)_4$	Helicate	11.4647(12)	[30]
$[\text{Ni}_2(\text{p-xpt})_3](\text{BF}_4)_4$ (3a)	Helicate	11.574(2)	This work
$[\text{Fe}_2(\text{p-xpt})_3](\text{BF}_4)_4$	Helicate	11.3912(11)	[30]
$[\text{Ru}_2(\text{p-xpt})_3](\text{BF}_4)_4$	Helicate	11.6368(9)	[35]
$[\text{Ni}_2(\text{p-xamt})_3](\text{NO}_3)_4$ (3b)	Helicate	11.899(2), 11.924(2)	This work

^a This complex is identical to $[\text{Fe}_2(m\text{-xpt})_3](\text{BF}_4)_4$, except that the central aromatic rings in the 2,6-pmpt ligands are 2,6-disubstituted pyridine rather than m -disubstituted benzene.

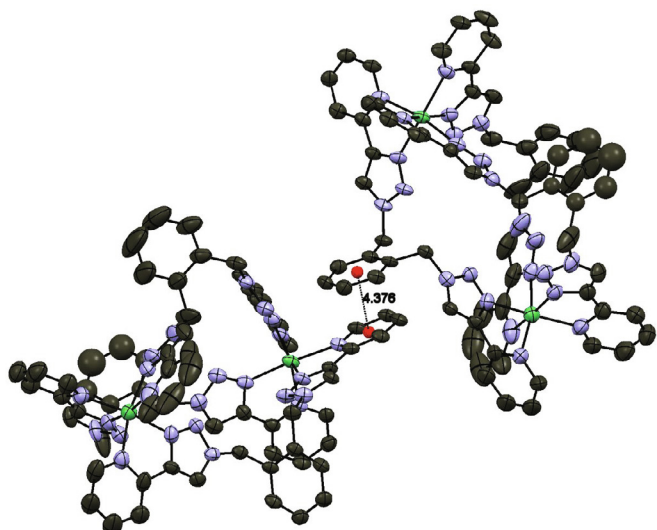


Fig. 5. Packing diagram for $[\text{Ni}_2(o\text{-xpt})_3]^{4+}$ (**1a**), showing the $\pi\text{-}\pi$ interactions between a phenylene ring of one complex and a pyridyl ring of an adjacent complex. Anions, hydrogen atoms, and solvent molecules have been removed for clarity.

pounds containing *ortho*-xylylene spacers (**1a** and **1b**) exhibit a similar folding of their ligands (Figs. 4 and 6). In both structures, one of the phenylene rings twists almost perpendicular to the Ni...Ni axis, while the other two rings are oriented along the axial direction. In the crystal structure of **1a**, adjacent molecules show a pyridyl-phenylene π interaction (centroid...centroid 4.38 Å) (Fig. 5). In the crystal structure of **1b**, the two phenylene groups lying along the internuclear axis interact with a nearby triazole ring with $\text{CH}\cdots\pi$ interactions (H...centroid distance ca. 2.7 Å). These intra- and intermolecular non-covalent interactions may contribute to the almost spherical shapes of the complexes (approximate overall diameter of 15 Å) (to H) with axial distance ranging from ~ 13 to 18 Å (Fig. 6).

The triple helical complexes with *para*-xylylene spacers (**3a** and **3b**) were found to be more cylindrical than their *ortho* counterparts (Fig. 6). The overall length of the molecules with *p*-xylylene spacers ranges from ca. 16 Å (**3b**) to 20 Å (**3a**) (H...H) while the diameters of the circumscribed cylinders in both structures are nearly 10 Å. The orientation of the three *p*-xylylene spacers is orthogonal in complex **3a** while two of them are in almost parallel orientation (with an inter-centroid distance of ca. 5.2 Å) in complex **3b**. The pyridyltriazole units between two adjacent helicates are associated in a head-to-tail arrangement (the pyridyl group of one molecule stacks over the triazole group of the other molecule) in **3a** with an average interplanar distance of ca. 4.2 Å. In addition, the hydrogen atom attached to C64 of pyridyl moiety of one helicate makes a close approach (3.763 Å) to the triazole N11 of another helicate. These intermolecular contacts are illustrated in Fig. 7. Petitjean and co-workers have reported such interactions in the structure of $[\text{Fe}_2(p\text{-xpt})_3](\text{BF}_4)_4$, but the distances are shorter ($\pi\text{-}\pi$ stacking, 3.52 Å; $\text{H}_{\text{py}}\cdots\text{N}_{(\text{triazole})}$, 2.66 Å) [30] than in the current complex.

Because complexes **1b** and **3b** are the first aminomethyltriazole-based helicates to be reported, we were interested in any structural differences between them and the pyridyltriazole complexes (**1a** and **3a**). The pyridyl groups (in **1a** and **3a**) and the aminomethyl groups (in **1b** and **3b**) are *fac*-oriented, so they could interfere sterically. In the aminomethyl complexes (**1b** and **3b**), the closest nonbonded contacts between the $-\text{CH}_2\text{NH}_2$ groups are $\text{NH}\cdots\text{HN}$, which average 2.72 ± 0.17 Å. This is larger than twice the H atom van der Waals radius (2.2–2.4 Å); thus, there are few or no repulsive interactions among the $-\text{CH}_2\text{NH}_2$ groups. On the

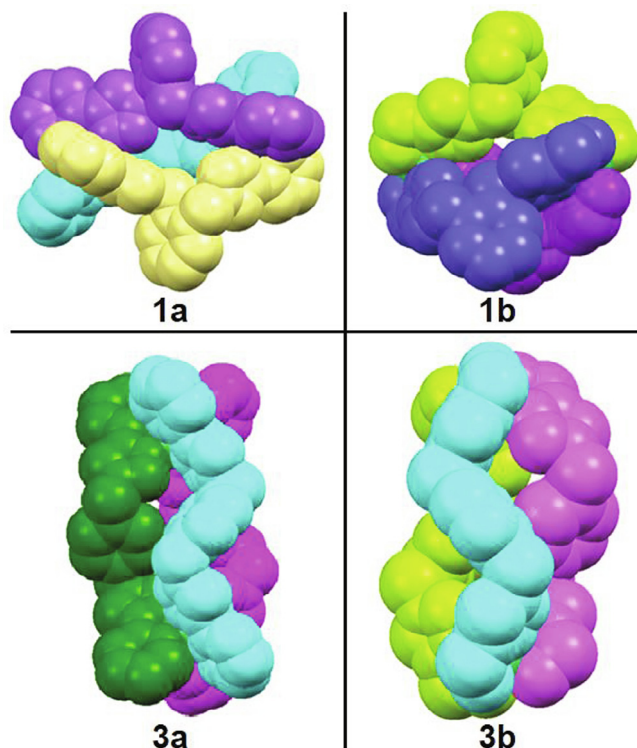


Fig. 6. Space-filling models of the molecular structures of the triple helicates. Different colors are used to distinguish the three different ligands in each structure. Anions, hydrogen atoms, and solvent molecules have been removed for clarity. **1a**, $[\text{Ni}_2(o\text{-xpt})_3]^{4+}$; **3a**, $[\text{Ni}_2(p\text{-xpt})_3]^{4+}$; **1b**, $[\text{Ni}_2(o\text{-xamt})_3]^{4+}$; **3b**, $[\text{Ni}_2(p\text{-xamt})_3]^{4+}$.

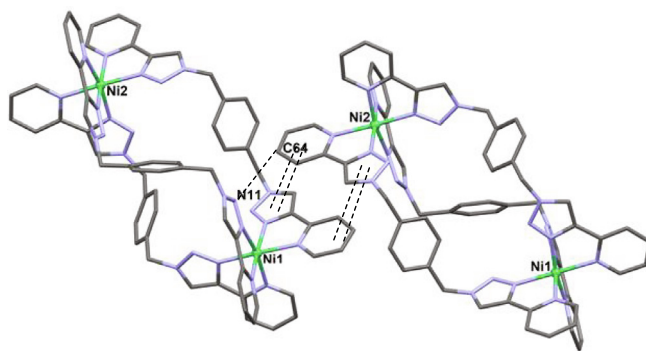


Fig. 7. Packing diagram for $[\text{Ni}_2(p\text{-xpt})_3](\text{BF}_4)_4$ (**3a**), showing intermolecular $\pi\text{-}\pi$ interactions. Anions, hydrogen atoms, and solvent molecules have been removed for clarity.

other hand, the pyridyl groups in **1a** and **3a** show $\text{C}\text{-H}\cdots\text{N}$ non-bonded distances of 2.77 ± 0.09 Å, approximately equal to the sum of the H and N van der Waals radii (2.65–2.75 Å). These contacts could lead to differences in N-Ni-N angles for the two ligands. However, the average $\text{N}(\text{pyridyl})\text{-Ni-N}(\text{pyridyl})$ angles in **1a** and **3a** ($95.7 \pm 2.3^\circ$) are not significantly larger than those for $\text{N}(\text{aminomethyl})\text{-Ni-N}(\text{aminomethyl})$ in **1b** and **3b** ($94.6 \pm 2.2^\circ$). Similarly, Ni-N(triazole) distances (2.061 ± 0.016 Å in all four structures) are shorter than either Ni-N(pyridyl) or Ni-N(aminomethyl), but there is little difference between the latter two (2.108 ± 0.016 and 2.115 ± 0.016 Å, respectively). This agrees with distances found in 6 previous examples of $[\text{Ni}_2(\text{2-aminomethylpyridine})_3]^{2+}$ structures: Ni-N(pyridyl), 2.099 ± 0.019 Å; Ni-N(aminomethyl), 2.115 ± 0.017 Å [46]. Therefore, despite their chemical differences, the aminomethyl and pyridyl ligating groups provide similar coordination environments in these helicates.

4. Conclusions

In order to understand the roles of spacer groups and chelating pockets in determining coordination behavior of ligands and dimensions of the overall complexes, we studied the complexation of Ni(II) with tetradentate *N*-donating ligands separated by xylylene spacers by altering two parameters: 1) the structure of the xylylene core (*o*-, *m*-, *p*-), and 2) the nature of the chelating groups. Pyridyltriazoles have been used extensively as coordination pockets in supramolecular chemistry. However, to the best of our knowledge, this is the first report of synthesis of tetradentate bis(aminomethyltriazole) ligands and their complexes. Regardless of the steric constraints of intra-ligand strands, all three isomeric xylylene spacers gave binuclear triple helical complexes. The complexes having an *o*-xylylene spacer gave roughly spherical shape with asymmetrically folded ligand strands, while the *p*-xylylene-bridged complexes are approximately cylindrical with a more symmetrical arrangement of ligands. Molecules with a common xylylene spacer have similar shapes, although the details of the solid-state packing of these complexes vary in a less predictable way.

CRediT authorship contribution statement

Uttam R. Pokharel: Conceptualization, Methodology, Investigation, Visualization, Writing - original draft, Writing - review & editing. **Jordan C. Theriot:** Methodology, Investigation. **Frank R. Fronczek:** Investigation, Formal analysis, Resources, Validation, Writing - review & editing. **Andrew W. Maverick:** Funding acquisition, Conceptualization, Visualization, Writing - review & editing.

Declaration of Competing Interest

The authors declare that they have no known competing financial interests or personal relationships that could have appeared to influence the work reported in this paper.

Acknowledgments

This research was supported in part by the Louisiana Board of Regents Support Fund (through the Louisiana EPSCoR project, NSF award number EPS-1003897) and Albemarle Corporation, and by the LSU Philip W. West Professorship. J. C. T. is grateful for partial support through the California Institute of Technology SURF program. The sponsors had no role in the design, execution, or publication of this work.

Appendix A. Supplementary data

CCDC 2010484, 2010486, 2010485, and 2010487 contain the supplementary crystallographic data for structures **1a**, **3a**, **1b**, and **3b**, respectively. These data can be obtained free of charge via <https://www.ccdc.cam.ac.uk/structures/> or from the Cambridge Crystallographic Data Centre, 12 Union Road, Cambridge CB2 1EZ, UK; fax: (+44) 1223-336-033; or e-mail: deposit@ccdc.cam.ac.uk. Supplementary data to this article can be found online at <https://doi.org/10.1016/j.poly.2020.114805>.

References

- [1] M. Albrecht, "Let's twist again"-double-stranded, triple-stranded, and circular helicates, *Chem. Rev.* 101 (2001) 3457–3497, <https://doi.org/10.1021/cr0103672>.
- [2] S.J. Dalgarno, N.P. Power, J.L. Atwood, Metallo-supramolecular capsules, *Coord. Chem. Rev.* 252 (2008) 825–841, <https://doi.org/10.1016/j.ccr.2007.10.010>.
- [3] M. Fujita, M. Tominaga, A. Hori, B. Therrien, Coordination assemblies from a Pd(II)-cornered square complex, *Acc. Chem. Res.*, 38 (2005) 369–378. doi: 10.1021/ar040153h.
- [4] M. Fujita, K. Umemoto, M. Yoshizawa, N. Fujita, T. Kusukawa, K. Biradha, Molecular paneling via coordination, *Chem. Commun.* (2001) 509–518, <https://doi.org/10.1039/b008684n>.
- [5] B.J. Holliday, C.A. Mirkin, Strategies for the construction of supramolecular compounds through coordination chemistry, *Angew. Chem., Int. Ed.*, 40 (2001) 2022–2043; doi: 10.1002/1521-3773(20010601)40:11<2022::AID-ANIE2022>3.0.CO;2-D.
- [6] T.R. Cook, P.J. Stang, Recent developments in the preparation and chemistry of metallacycles and metallacages via coordination, *Chem. Rev.* 115 (2015) 7001–7045, <https://doi.org/10.1021/cr5005666>.
- [7] C.R.K. Glasson, L.F. Lindoy, G.V. Meehan, Recent developments in the d-block metallo-supramolecular chemistry of polypyridyls, *Coord. Chem. Rev.* 252 (2008) 940–963, <https://doi.org/10.1016/j.ccr.2007.10.013>.
- [8] C. Zhao, J. Geng, L. Feng, J. Ren, X. Qu, Chiral metallo-supramolecular complexes selectively induce human telomeric G-quadruplex formation under salt-deficient conditions, *Chem. - Eur. J.* 17 (2011) 8209–8215, <https://doi.org/10.1002/chem.201100272>.
- [9] H. Yu, X. Wang, M. Fu, J. Ren, X. Qu, Chiral metallo-supramolecular complexes selectively recognize human telomeric G-quadruplex DNA, *Nucleic Acids Res.* 36 (2008) 5695–5703, <https://doi.org/10.1093/nar/gkn569>.
- [10] C. Ducani, A. Leczkowska, N.J. Hodges, M.J. Hannon, Noncovalent DNA-binding metallo-supramolecular cylinders prevent DNA transactions in vitro, *Angew. Chem., Int. Ed.*, 49 (2010) 8942–8945. doi: 10.1002/anie.201004471.
- [11] L. Cardo, V. Sadovnikova, S. Phongtongpasuk, N.J. Hodges, M.J. Hannon, Arginine conjugates of metallo-supramolecular cylinders prescribe helicity and enhance DNA junction binding and cellular activity, *Chem. Commun.*, 47 (2011) 6575–6577. doi: 10.1039/c1cc11356a.
- [12] A. Oleksy, A.G. Blanco, R. Boer, I. Uson, J. Aymami, A. Rodger, M.J. Hannon, M. Coll, Molecular recognition of a three-way DNA junction by a metallosupramolecular helicate, *Angew. Chem. Int. Ed.*, 45 (2006) 1227–1231. doi: 10.1002/anie.200503822.
- [13] H. Yu, M. Li, G. Liu, J. Geng, J. Wang, J. Ren, C. Zhao, X. Qu, Metallosupramolecular complex targeting an α/β discordant stretch of amyloid β peptide, *Chem. Sci.* 3 (2012) 3145–3153, <https://doi.org/10.1039/c2sc20372c>.
- [14] R. Krämer, J.-M. Lehn, A. De Cian, J. Fischer, Self-assembly, structure, and spontaneous resolution of a trinuclear triple helix from an oligobipyridine ligand and Ni^{II} ions, *Angew. Chem. Int. Ed. Engl.* 32 (1993) 703–706, <https://doi.org/10.1002/anie.199307031>.
- [15] M.-H. Shu, C.-Y. Duan, W.-Y. Sun, Y.-J. Fu, D.-H. Zhang, Z.-P. Bai, W.-X. Tang, Synthesis, structure and characterization of novel nickel(II) and iron(II) complexes with a 5,5'-bis[2-(2,2'-bipyridin-6-yl)-ethyl]-2,2'-bipyridine ligand, *J. Chem. Soc., Dalton Trans.*, (1999) 2317–2322. doi: 10.1039/A901835B.
- [16] C.R.K. Glasson, G.V. Meehan, C.A. Motti, J.K. Clegg, P. Turner, P. Jensen, L.F. Lindoy, New nickel(II) and iron(II) helicates and tetrahedra derived from expanded quaterpyridines, *Dalton Trans.*, 40 (2011) 10481–10490. doi: 10.1039/c1dt10667h.
- [17] J.D. Crowley, P.H. Bandeen, A multicomponent CuAAC "click" approach to a library of hybrid polydentate 2-pyridyl-1,2,3-triazole ligands: new building blocks for the generation of metallosupramolecular architectures, *Dalton Trans.*, 39 (2010) 612–623. doi: 10.1039/B911276F.
- [18] L. Liang, D. Astruc, The copper(I)-catalyzed alkyne-azide cycloaddition (CuAAC) "click" reaction and its applications. An overview, *Coord. Chem. Rev.* 255 (2011) 2933–2945, <https://doi.org/10.1016/j.ccr.2011.06.028>.
- [19] A.W. Maverick, S.C. Buckingham, Q. Yao, J.R. Bradbury, G.G. Stanley, Intramolecular coordination of bidentate Lewis bases to a cofacial binuclear copper(II) complex, *J. Am. Chem. Soc.* 108 (1986) 7430–7431, <https://doi.org/10.1021/ja00283a060>.
- [20] C. Pariya, F.R. Fronczek, A.W. Maverick, Bis(*o*-phenylenebis(acetylacetonato)) dicopper(II): A strained copper(II) dimer exhibiting a wide range of colors in the solid state, *Inorg. Chem.* 50 (2011) 2748–2753, <https://doi.org/10.1021/ic101641r>.
- [21] C. Pariya, C.R. Sparrow, C.-K. Back, G. Sandí, F.R. Fronczek, A.W. Maverick, Copper β -diketonate molecular squares and their host-guest reactions, *Angew. Chem. Int. Ed.* 46 (2007) 6305–6308, <https://doi.org/10.1002/anie.200701252>.
- [22] U.R. Pokharel, F.R. Fronczek, A.W. Maverick, Cyclic pyridyltriazole-Cu(II) dimers as supramolecular hosts, *Dalton Trans.*, 42 (2013) 14064–14067. doi: 10.1039/C3DT52208C.
- [23] U.R. Pokharel, F.R. Fronczek, A.W. Maverick, Reduction of carbon dioxide to oxalate by a binuclear copper complex, *Nat. Commun.* 5 (2014) 5883, <https://doi.org/10.1038/ncomms6883>.
- [24] A.W. Maverick, F.L. Klavetter, Cofacial binuclear copper complexes of a bis(β -diketonate) ligand, *Inorg. Chem.*, 23 (1984) 4129–4130. doi: 10.1021/ic00193a005.
- [25] J.D. Crowley, D.A. McMorran, "Click-triazole" coordination chemistry: exploiting 1,4-disubstituted-1,2,3-triazoles as ligands, in: J. Košmrlj (Ed.), *Click Triazoles, Topics in Heterocyclic Chemistry*, 28, Springer-Verlag, Berlin, Heidelberg, 2012, pp. 31–83, https://doi.org/10.1007/7081_2011_67.
- [26] H. Struthers, D. Viertl, M. Kosinski, B. Spingler, F. Buchegger, R. Schibli, Charge dependent substrate activity of C3' and N3 functionalized, organometallic technetium and rhenium-labeled thymidine derivatives toward human thymidine kinase 1, *Bioconjugate Chem.* 21 (2010) 622–634, <https://doi.org/10.1021/bc900380n>.
- [27] A. Maissonial, P. Serafin, M. Traïkia, E. Debiton, V. Théry, D.J. Aitken, P. Lemoine, B. Viossat, A. Gautier, Click chelators for platinum-based anticancer drugs, *Eur. J. Inorg. Chem.* 2008 (2008) 298–305, <https://doi.org/10.1002/ejic.200700849>.

- [28] A. Chevry, M.-L. Teyssot, A. Maisonia, P. Lemoine, B. Viossat, M. Traïkia, D.J. Aitken, G. Alves, L. Morel, L. Nauton, A. Gautier, Click chelators – the behavior of platinum and palladium complexes in the presence of guanosine and DNA, *Eur. J. Inorg. Chem.* (2010) (2010) 3513–3519, <https://doi.org/10.1002/ejic.201000183>.
- [29] N. Wu, C.F.C. Melan, K.A. Stevenson, O. Fleischel, H. Guo, F. Habib, R.J. Holmberg, M. Murugesu, N.J. Mosey, H. Nierengarten, A. Petitjean, Systematic study of the synthesis and coordination of 2-(1,2,3-triazol-4-yl)-pyridine to Fe(II), Ni(II) and Zn(II); ion-induced folding into helicates, mesocates and larger architectures, and application to magnetism and self-selection, *Dalton Trans.*, 44 (2015) 14991–15005. doi: 10.1039/C5DT00233H.
- [30] K.A. Stevenson, C.F.C. Melan, O. Fleischel, R. Wang, A. Petitjean, Solid-state self-assembly of triazolylpyridine-based helicates and mesocate: control of the metal–metal distances, *Cryst. Growth Des.*, 12 (2012) 5169–5173. doi: 10.1021/cg301197w.
- [31] D. Schweinfurth, J. Krzystek, I. Schapiro, S. Demeshko, J. Klein, J. Telsler, A. Ozarowski, C.Y. Su, F. Meyer, M. Atanasov, F. Neese, B. Sarkar, Electronic structures of octahedral Ni(II) complexes with “click” derived triazole ligands: a combined structural, magnetometric, spectroscopic, and theoretical study, *Inorg. Chem.*, 52 (2013) 6880–6892. doi: 10.1021/ic3026123.
- [32] J.P. Byrne, J.A. Kitchen, O. Kotova, V. Leigh, A.P. Bell, J.J. Boland, M. Albrecht, T. Gunnlaugsson, Synthesis, structural, photophysical and electrochemical studies of various d-metal complexes of btp [2,6-bis(1,2,3-triazol-4-yl)pyridine] ligands that give rise to the formation of metallo-supramolecular gels, *Dalton Trans.*, 43 (2014) 196–209. doi: 10.1039/C3DT52309H.
- [33] B. Jana, L. Cera, B. Akhuli, S. Naskar, C.A. Schalley, P. Ghosh, Competitive transmetalation of first-row transition-metal ions between trinuclear triple-stranded side-by-side helicates, *Inorg. Chem.*, 56 (2017) 12505–12513. doi: 10.1021/acs.inorgchem.7b01980.
- [34] H. Zhao, X. Li, J. Wang, L. Li, R. Wang, Synthesis and crystal structures of coordination complexes containing Cu₂L₂ Units and their application in luminescence and catalysis, *ChemPlusChem* 78 (2013) 1491–1502, <https://doi.org/10.1002/cplu.201300249>.
- [35] S.V. Kumar, W.K.C. Lo, H.J.L. Brooks, J.D. Crowley, Synthesis, structure, stability and antimicrobial activity of a ruthenium(II) helicate derived from a bis-bidentate “click” pyridyl-1,2,3-triazole ligand, *Inorg. Chim. Acta*, 425 (2015) 1–6. doi: 10.1016/j.ica.2014.10.011.
- [36] D. Sykes, M.D. Ward, Visible-light sensitisation of Tb(III) luminescence using a blue-emitting Ir(III) complex as energy-donor, *Chem. Commun.*, 47 (2011) 2279–2281. doi: 10.1039/C0CC04562D.
- [37] A. Najjar, I. Tidmarsh, M. Ward, Lead(II) complexes of bis- and tris-bidentate compartmental ligands based on pyridyl-pyrazole and pyridyl-triazole fragments: coordination networks and a discrete dimeric box, *CrystEngComm* 12 (2010), <https://doi.org/10.1039/c0ce00176g>.
- [38] S.V. Kumar, W.K.C. Lo, H.J.L. Brooks, L.R. Hanton, J.D. Crowley, Antimicrobial properties of mono- and di-*fac*-rhenium tricarbonyl 2-pyridyl-1,2,3-triazole complexes, *Aust. J. Chem.* 69 (2016) 489–498, <https://doi.org/10.1071/CH15433>.
- [39] S.K. Vellas, J.E.M. Lewis, M. Shankar, A. Sagatova, J.D.A. Tyndall, B.C. Monk, C.M. Fitchett, L.R. Hanton, J.D. Crowley, [Fe₂L₃]⁴⁺ cylinders derived from bis (bidentate) 2-pyridyl-1,2,3-triazole “click” ligands: synthesis, structures and exploration of biological activity, *Molecules* 18 (2013) 6383–6407, <https://doi.org/10.3390/molecules18066383>.
- [40] V. Haridas, S. Sahu, P. Venugopalan, Halide binding and self-assembling behavior of triazole-based acyclic and cyclic molecules, *Tetrahedron* 67 (2011) 727–733, <https://doi.org/10.1016/j.tet.2010.11.078>.
- [41] N. Gigant, E. Claveau, P. Bouyssou, I. Gillaizeau, Diversity-oriented synthesis of polycyclic diazine scaffolds, *Org. Lett.* 14 (2012) 844–847, <https://doi.org/10.1021/ol203364b>.
- [42] Bruker, SADABS (2001), Bruker AXS Inc.; Madison, Wisconsin, USA.
- [43] G.M. Sheldrick, Crystal structure refinement with SHELXL, *Acta Crystallogr. Sect. C: Struct. Chem.*, 71 (2015) 3–8. doi: 10.1107/s2053229614024218.
- [44] A.L. Spek, PLATON SQUEEZE: a tool for the calculation of the disordered solvent contribution to the calculated structure factors, *Acta Crystallogr. Sect. C: Struct. Chem.*, 71 (2015) 9–18. doi: 10.1107/s2053229614024929.
- [45] M. Albrecht, How do they know? Influencing the relative stereochemistry of the complex units of dinuclear triple-stranded helicate-type complexes, *Chem. Eur. J.*, 6 (2000) 3485–3489. doi: 10.1002/1521-3765(20001002)6:19<3485::aid-chem3485>3.0.co;2-3.
- [46] C.R. Groom, I.J. Bruno, M.P. Lightfoot, S.C. Ward, The Cambridge structural database, *Acta Crystallogr. Sect. B: Struct. Sci.* 72 (2016) 171–179, <https://doi.org/10.1107/S2052520616003954>.